Reddy *et al. J Wireless Com Network* (2022) 2022:57
https://doi.org/10.1186/s13638-022-02133-3

EURASIP Journal on Wireless Communications and Networking

RESEARCH Open Access

Uplink coverage enhancements for extremely large-cell sites

M. Pavan Reddy*, G. Koteswara Rao, D. Harish Kumar, K. Subhash, SaiDhiraj Amuru and Kiran Kuchi

*Correspondence: ee14resch11005@iith.ac.in

Department of Electrical Engineering, IIT Hyderabad, Hyderabad, India

Abstract

In urban areas, the network operators deploy small-cell sites and install a large number of base stations to support densely populated cellular users. A similar small-cell deployment in rural areas is not feasible for the operators, as it will significantly increase the capital expenditure, and the return on the investment will also be comparatively lower. Hence, the most feasible way to provide cellular connectivity to rural areas is the deployment of large-cell sites. However, the technology developed for International Mobile Telecommunications (IMT)-Advanced standard (or 4G) was evaluated for an inter-site distance of 1.732 km, making the large-cell connectivity required for rural areas an afterthought. For cellular last-mile rural connectivity to be a reality through IMT-2020 (or 5G), the key is to have future technologies supporting large cells. In large-cell sites, the users experience comparatively more path loss, and thus, have poor signal coverage. Further, compared to downlink, the transmission power in uplink is limited, and therefore, uplink transmissions define the coverage of the communication system. Motivated by this, we propose several coverage solutions for uplink, considering an extremely large-cell site scenario. We initially analyze the received signal-to-noise ratio with 4G/5G systems at various distances based on the link budget evaluation. At larger inter-site distances, we show that it is infeasible to achieve cellular coverage with the current 4G/5G specifications. We then propose enhancements related to the waveform, modulation and coding schemes, resource allocation, and power control mechanisms. We evaluate the proposed enhancements through system- and link-level simulations, and show a significant improvement in the coverage for cell-edge users. We also show that our proposed enhancements achieve close to two times the improvement in the network capacity when compared to the currently available 5G specifications.

Keywords: Coverage, CQI, MCS, Power control, Resource allocation, Uplink

1 Introduction

Digital connectivity is an important driver for modern day economies, and in the current times, it is a quintessential necessity for day-to-day living. The mobile connectivity has become popular with the advent of 4G-long-term evolution (LTE), a wireless standard that vastly improved the connectivity speeds and reduced the price per bit. Increasing capacity, reliability, and higher data rates have been the main focus of the cellular industry, and the new 5G-New Radio (5G-NR) standard is a reflection of this paradigm.

Massive multi-input-multi-output (MIMO) has been introduced in the new cellular standard to increase the network capacity. This increased capacity translates to a better user experience and better throughput, leading to higher average revenue per user. An important and practical manner for achieving higher capacity (and per-user throughput) that is used by operators is to reduce the cell size. Smaller cell sizes lead to a higher bandwidth per user in the downlink, thereby increasing the per-user throughput. A smaller cell would also increase the received signal power by the users, thereby enabling higher modulations for the cell-edge users, thus further enhancing the data rates. Hence, in the urban areas, we see a large number of the base station (BS) towers that provide the necessary infrastructure to support a large number of cellular users.

In contrast, mobile broadband connectivity in rural areas is not very encouraging. This is mainly because of the huge capital expenditure (CapEx) needed to establish and maintain cellular mobile towers in rural areas. And also, the return on investment might be lower as compared to the cities. However, in developing countries like India, most of the population is rural, and the availability of broadband connectivity is critical for bridging the digital divide. To improve rural connectivity, the government of India has taken the initiative to provide optical fiber connectivity to 250,000 gram-panchayats (GPs) across India [1]. However, with a possible BS deployment at each such GP, the last-mile connectivity is still an issue because of the large geographical area. In Fig. 1, we present a cumulative distribution function (CDF) of maximum distance between a village and a possible BS deployment (at GP) [2]. From Fig. 1, to provide 95% coverage to the rural villages in India, the minimum feasible inter-site distance is 12 km. Most of the technology developed for IMT-advanced (4G-LTE) was designed and evaluated for an inter-site distance of 1.732 km. Such small-cell deployment will require the network operator to install a BS in every village, which significantly increases the CapEx costs and is impractical. Hence, the villages in developing countries such as India were severely under-served, or the cost of the rural deployment was significantly high. For cellular last-mile rural connectivity to be a reality through IMT-2020 (5G-NR), the key is to have future technologies supporting large cells.

In large-cell sites, the users are at a large distance from the BS, and thus, experience more path loss. Further, in sub-6 GHz range, as compared to LTE, 5G-NR is expected to

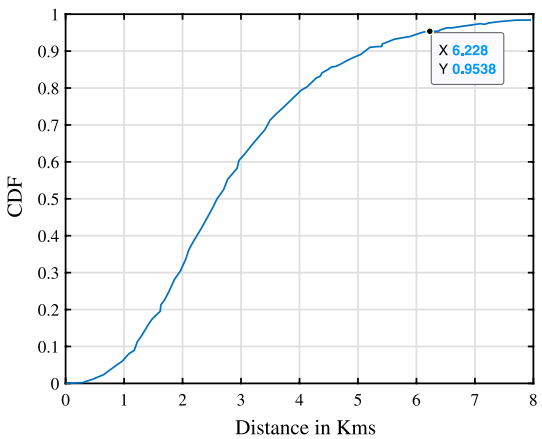

Fig. 1 CDF of maximum distance between a village and a feasible BS in rural Indian scenario

be deployed in higher frequencies like 4 GHz. Note that with higher frequencies as well, the users will observe comparatively more path loss. Hence, with higher operating frequencies and large inter-site distances, there is a significant impact on the cell coverage. Thus, large-cell sites will require novel enhancements to ensure successful communication. Till the recent releases of 3GPP specifications, the coverage enhancement has been addressed only in the context of machine-type communications and was not treated for the enhanced mobile broadband services [3]. 3GPP has considered coverage enhancements in 5G-NR as a new work area for the Release 17 specifications [4]. However, there has been very little work on the design aspects of cellular systems for large cells. We need novel physical layer procedures to address the issue, and further, these novel ideas require changes to various parts of the current specifications accordingly. These are the key motivations for this work.

When compared to the transmission power of 43 dBm in the downlink, the transmission power in the uplink is limited to 23 dBm at the user equipment (UE) [5] because of hardware limitations and regulatory constraints. Thus, uplink transmissions define the coverage area. Hence, in this paper, we present proposals for coverage enhancements in the uplink for large-cell sites. The main contributions of this paper are as follows.

- We present the link budget analysis for large-cell sites considering the rural scenario and show that at such larger inter-site distances, it is infeasible to achieve cellular coverage with the current 5G-NR specifications.
- We show that $\pi/2$-BPSK with spectrum shaping filter has a significantly low peak-to-average power ratio (PAPR). We then propose to use $\pi/2$-BPSK waveform for enhanced coverage in large-cell sites.
- We propose novel transmit power boosting and resource allocation techniques to improve the SNRs of cell-edge users.
- We also define new modulation and coding scheme entries for the users operating at poor SNRs.
- We propose a transport-block scaling mechanism to improve the coverage of the cell-edge users.
- Through system- and link-level simulations, we show that the proposed enhancements significantly improve the cell coverage.

The rest of the paper is organized as follows. In Sect. 2, we present the related work in the literature. Section 3 presents the link budget simulations and coverage related analysis. In Sect. 4, we propose various enhancements for large-cell scenario. Section 5 presents system-level simulations and results. In Sect. 6, we present conclusion and discuss the possible future work.

2 Related work

In [6], authors have analyzed the coverage enhancements features of machine-type communications (MTC) and have provided link and system-level evaluation for various physical layer channels. An optimal selection of repetitions, resource allocation, modulation, and coding schemes for enhancing the coverage in NB-IoT has been presented in [7]. In [8], authors have discussed all the coverage enhancement techniques

of machine-type communications in detail. A design of the narrowband communication system on the unlicensed spectrum has been discussed in [9]. The authors have shown significant improvements in coverage of the devices with the proposed design. In [10, 11], authors have presented constellation and channel decoder-based improvements to enhance the coverage of MTC devices. However, all these works are in the context of low power wide area network technology and cannot be directly applied to the enhanced mobile broadband (eMBB) services.

The coverage enhancement evaluation and the network performance results with pre-5G deployment in the sub-6 GHz frequency range have been presented in [12]. In [13], authors have investigated the coverage enhancement features like hybrid-ARQ and TTI bundling for improving the voice over LTE performance. In [14], authors have proposed digital beamforming techniques for 5G-NR deployed in the sub-6 GHz range and have shown an improvement in the coverage of the users. However, to the best of our knowledge, none of the existing works has addressed the issue of coverage enhancement with eMBB for large-cell sites. 3GPP has also considered this issue as a work area for the Release 17 specifications [4]. Hence, in this paper, we propose various solutions to improve the coverage for large-cell sites.

3 Uplink coverage analysis in large-cell sites

In this section, we initially discuss a newly introduced rural channel model for low mobility large-cell scenario, and then, we present link budget analysis for the large-cell sites.

3.1 Low-mobility large-cell configuration

International telecommunications union (ITU) is an international body that defines the capabilities and requirements of a wireless technology and ratifies the same for wireless standards developed by other standardization bodies like the 3GPP. Currently, ITU defines indoor-hotspot, dense-urban, rural, mMTC, and URLLC as the test case environments. Indoor-hotspot and dense-urban test environments focus on urban scenarios and target very high data rates. mMTC targets IoT applications, while URLLC focuses on low latency reliable applications [15]. 3GPP also uses these channel models and test cases for the purpose of evaluation and technology development.

Till IMT-2020, the rural models consider vehicles moving at high speed of 120 kmph and inter-site distance not greater than 1732 m. However, in IMT-2020, a new test case named low-mobility-large-cell (LMLC) was introduced as a sub-configuration of rural test case. This new configuration focuses on low-mobility users (a mix of the pedestrian with speeds less than 3 kmph and vehicles at 30 kmph) and an inter-site distance of 6 km. Unlike other rural cases, LMLC does not focus on high-speed mobility. In addition to the test configuration, a new channel model was introduced for the LMLC rural scenario to aid in the simulation of large cells, which is valid until 21 kms. However, as mentioned in [16], we assume that the same LMLC path loss is valid beyond 21 kms and use it in our link budget analysis and the system-level evaluation.

3.2 Link budget analysis

The SNR observed by a user defines the coverage in any wireless communication system. In large-cell sites, with the increasing distance, the impact of the interference decreases, and thus, the transmit power and thermal noise dominate the cell capacity. In such scenarios, the performance observed in the link budget is close to the real life. Hence, in this section, we present the link budget evaluation and analyze the operating SNRs of users in a large-cell site.

The parameters considered for link budget simulation are presented in Table 1. We consider a carrier frequency of 700 MHz with 16-element antenna configuration at the BS [18]. Typically, the antenna configuration is defined as $M \times N \times P$, where M and N are the antenna elements in the horizontal and vertical directions, respectively, and P represents the polarization of the antenna elements. We present an appropriate antenna array in Table 1 as per [18]. While evaluating the downlink, we assume that the BS transmit power is used across entire 10 MHz bandwidth. In case of uplink, we consider a worst-case scenario of one resource block allocation and use entire transmit power on one resource block. In this paper, we target our simulations for an inter-site distance (ISD) of 30 kms [16]. However, note that the analysis in this paper can be extended to any configuration of carrier frequencies, antenna configurations, and inter-site distances.

The path loss and antenna gains are the key factors that significantly impact the SNR of a user and are heavily dependent on the user location. The maximum antenna gain (Ag) in the boresight direction is 8 dB [17], but the antenna gain varies with the user position. In a worst-case scenario, with a sector of 120°, a user can be located at ±60°. Hence, for the analysis, we consider the antenna gain at ±60° from the boresight, which results in Ag = −2 dB [17]. Further, the shadow fading is dependent on line of sight (LoS)/non-LoS (NLoS) scenario. The standard deviation for shadow fading in LoS and NLoS scenarios is 6 dB and 8 dB, respectively [15]. The path loss models follow a log-normal distribution, and hence, at 95% of the CDF, the distribution has the value equal to 1.645 times the standard deviation. Considering a 95% coverage for

Table 1 Link budget simulation parameters

Parameters	Value
Carrier frequency (f_c)	700 MHz
Antenna at BS (N_{BS})	$[4 \times 2 \times 2] = 16$
Antennae at UE (N_{UE})	2
Path loss model	RMa-LMLC (ITU M.2412)
Transmit power (Pt_{BS}/Pt_{UE})	46 dBm/23 dBm
Bandwidth while evaluating downlink	10 MHz
Bandwidth while evaluating uplink	1 resource block (180 KHz)
Sub-carrier spacing	15 KHz
Noise power density	−174 dBm/Hz
Noise figure (NF)	5 dB
Maximum BS antenna element gain (Ag)	8 dB
UE height (h_{UT})	1.5 m
BS height (h_{BS})	35 m
Antenna pattern	TR 36.873 [17]

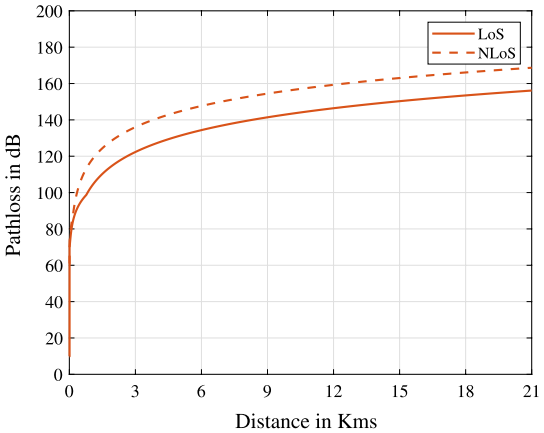

Fig. 2 Path loss versus distance for the simulation assumptions in Table 1

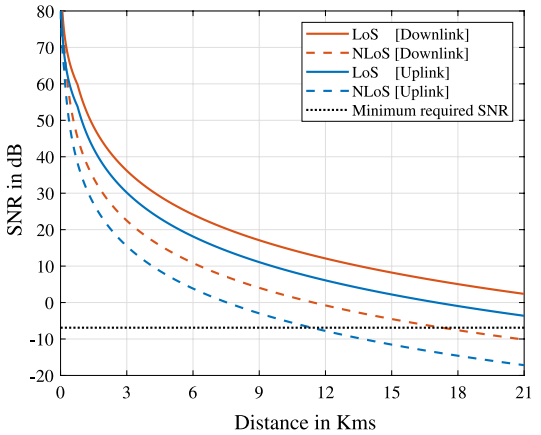

Fig. 3 SNR versus distance for the simulation assumptions in Table 1

calculating the maximum shadow fading margin, we have SF $= 1.645 \times 6 = 9.87$ dB and $1.645 \times 8 = 13.16$ B for LoS and NLoS scenarios, respectively.

We then calculate the SNR as follows.

$$\begin{aligned} \text{SNR} = {} & \text{Pt}_{\text{UE}} + \text{Ag} + 10 \times \log_{10}(N_{\text{BS}} \times N_{\text{UE}}) \\ & - \text{PL} - \text{SF} - [N_0 + \text{NF}] \end{aligned} \tag{1}$$

where PL is dependent on distance and is calculated as per RMa-LMLC path loss model presented in [15]. SF, Ag represent the shadow fading, antenna gain, respectively, and are calculated as mentioned earlier. N_{BS}, N_{UE} represent the number of antenna elements at the BS, UE, respectively, and are presented in Table 1. Apart from the basic antenna element gain Ag, the factor $10\log_{10}(N_{\text{BS}}N_{\text{UE}})$ captures the maximum additional gain that can be achieved with the total number of antenna elements. N_0, NF represent the noise and noise figure, respectively. All the parameters are considered in dB scale.

In Figs. 2 and 3, we present the variation of path loss and SNR with the distance. As shown in Fig. 2, the path loss increases with an increase in the distance, and the users in NLoS experience more path loss as compared to LoS. With an ISD = 30 km, the

maximum distance of any user from the BS is $\frac{\text{ISD}}{\sqrt{3}} = 17.325$ km. As shown in Table 3, the current LTE/NR specifications require a minimum operational SNR of −6.9 dB. In [19], the authors have presented a summary of link-level evaluation by various industrial operators and have shown that a minimum SNR of −6 dB is required to decode the control channel in LTE. From Fig. 3, at an ISD of 30 km, the downlink SNRs are in the feasible range for communication, whereas the uplink SNRs are as low as −15 dB. Even though only one resource block is considered for the transmission in uplink, the SNRs are very low because of the limited transmit power at the user.

1 ***Remark***

Thus, uplink transmissions define the coverage of large-cell sites, and it is infeasible to achieve cellular coverage with the current LTE/NR specifications. To address the issue, in this paper, we present various enhancements to the waveform, modulation and coding schemes, resource allocation, and power control mechanisms to achieve communication at these long distances.

Next, we explain our proposed enhancements in detail.

4 Proposals for uplink coverage enhancement

In this section, we propose various solutions to enhance the uplink coverage and provide the implementation details for the same.

4.1 Proposed waveform

In a cellular network, as compared to the downlink transmission power of 43 dBm at the BS, the uplink transmission power at the user terminal is limited to 23 dBm. This limitation is mainly because of the battery size at the user terminal and the regulatory constraints. Hence, in the uplink, the limited power has to be carefully utilized to enhance coverage. Considering these battery constraints, in LTE, instead of a regular OFDM, a discrete Fourier transform spread OFDM (DFT-s-OFDM) is used for the uplink transmissions. The PAPR with DFT-s-OFDM is less compared to the OFDM signal. Thus, the user terminal can have a less power amplifier back-off and transmit at higher signal power.

Based on a similar approach, in this section, we propose to use low PAPR $\pi/2$-BPSK waveform to enhance the uplink coverage in large-cell sites. In 5G-NR, along with the QAM modulations of order (4, 16, 64, 256), $\pi/2$-BPSK is supported in the uplink. $\pi/2$-BPSK is obtained by phase rotating the every odd BPSK symbol by $\pi/2$ degrees as shown below [20].

$$x_{\pi/2}(m) = \frac{1+j}{\sqrt{2}}.e^{j(m \bmod 2)}.x(m), \quad m \in [0, \ldots, M-1] \tag{2}$$

where x is a BPSK sequence of length M, and $x_{\pi/2}$ is corresponding $\pi/2$-BPSK sequence. The $\pi/2$-BPSK modulation has a similar constellation to that of QPSK. However, note that only one bit is transmitted with $\pi/2$-BPSK. As per the design of $\pi/2$-BPSK in (2), we find no zero cross-overs, and hence, the PAPR is comparatively less. When we introduce

Fig. 4 Implementation of $\pi/2$-BPSK with spectrum shaping

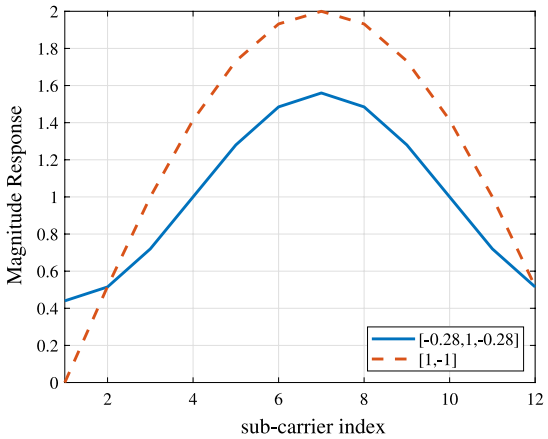

Fig. 5 Magnitude response of various spectral shaping filters

an appropriate spectrum shaping filter on the $\pi/2$-BPSK modulated data, we see a further decrease in the PAPR. In the frequency domain, the spectrum shaping can be implemented like a precoder with weights $W_f = D_M w_t$, where D_M represents the DFT matrix and w_t represents the time-domain impulse response of the spectrum shaping filter [21]. A comparison of the magnitude response of spectrum shaping filter with coefficients $[1, -1]$ and $[-0.28, 1, -0.28]$ is presented in Fig. 5.

A transmitter chain for $\pi/2$-BPSK with spectrum shaping filter is presented in Fig. 4. Initially, the data are modulated using BPSK scheme, and then, the $\pi/2$ rotation is performed on every odd BPSK symbol. The data are then transmitted through a spectrum shaping filter. The resultant data after spectrum shaping are passed through a DFT-s-OFDM chain. We have evaluated the PAPR for various modulation schemes with DFT-s-OFDM, and a complementary cumulative distribution function (CCDF) for the same is presented in Fig. 6. The $\pi/2$-BPSK modulation has significantly less PAPR when compared to the other standard modulation schemes. Further, with spectrum shaping, at 1% CCDF, we observe close to 3 dB difference when compared to the QPSK modulation scheme.

In Table 2, for a power amplifier that saturates at 25 dBm, we present the maximum possible transmit power with various modulation schemes [22] to reach the allowed adjacent channel leakage ratio (ACLR) limit of -30 dBm as per 3GPP specifications. It can be observed that $\pi/2$-BPSK with spectrum shaping can be transmitted at 3 dB high power as compared to the QPSK modulation scheme.

In an extremely large cell, as presented earlier in link budget analysis (in Sect. 3.2), the SINRs observed for an ISD $= 30$ km are as low as -15 dB.

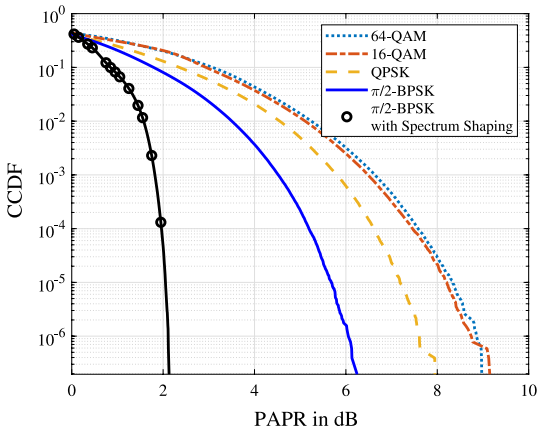

Fig. 6 CCDF of PAPR with various modulation schemes

Table 2 Tx power and ACLR comparison for various modulation schemes [22]

Scheme	Tx power [dBm]	ACLR
Random OFDM signal	19.1	−30.4
QPSK	21.7	−30.86
$\pi/2$-BPSK	23	−30.5
$\pi/2$-BPSK with spectrum shaping	24.8	−32.7

1 ***Remark***

Hence, in such scenarios, the user terminal can use $\pi/2$-BPSK with spectrum shaping, transmit at comparatively high power, and achieve better coverage.

Next, we explain a novel power boosting and allocation procedures for the uplink in a large-cell scenario.

4.2 Proposed power boosting and resource allocation

In this section, we initially explain the existing power control mechanism in the uplink and then propose the power boosting and resource allocation procedures.

4.2.1 Power control

The same time–frequency resource elements are allocated for various users across multiple sectors because of the frequency reuse. The transmission of one user will cause interference to the other users. Hence, there is a need for a mechanism that ensures the users closer to the BS transmit with minimal power and cause less interference to the users in other sectors. This is achieved by the uplink power control mechanism in 4G-LTE/5G-NR systems. The power control makes sure that the users transmit with adequate power, minimize interference for the other users in the

network, and maximize the user equipment's battery life. As per 3GPP specifications [23], the user equipment sets the transmit power P based on the following formula,

$$P = \min\{P_{\max}, 10\log_{10} N_{\mathrm{RB}} + P_0 + \alpha \mathrm{PL} + f(\delta_i) + \delta_{\mathrm{MCS}}\} \tag{3}$$

where $P_{\max}$ is the maximum power that a user can transmit, N_{RB} is the number of resource blocks that a user has to transmit the data, P_0 is a cell/user-specific parameter that considers the average interference in the network and the target signal strength from the user, PL is the path loss of the user, α is the factor for the fractional power control, and $f(\delta_i)$ and δ_{MCS} are the closed-loop power control parameters. Equation (3) is termed as a closed-loop power control because a BS decides $f(\delta_i)$ and δ_{MCS} based on the feedback received from the user. An open-loop version of the power control is defined as follows,

$$P = \min\{P_{\max}, 10\log_{10} N_{\mathrm{RB}} + P_0 + \alpha \mathrm{PL}\} \tag{4}$$

In (4), there is no user feedback, and the transmit power is completely defined by the BS based on P_0 and N_{RB}.

4.2.2 Power boosting

As presented in Sect. 4.1, the PAPR of QPSK is high compared to $\pi/2$-BPSK. Thus, a power amplifier designed for QPSK can transmit $\pi/2$-BPSK with additional power, as it can have less back-off with $\pi/2$-BPSK. This power boosting can be realized by adding δ_{boost} to P in (4) whenever the user is transmitting $\pi/2$-BPSK. Further, even after this power boosting, the average transmit power over a time duration should be same. Hence, based on the time division duplexing (TDD) configuration, considering the active uplink sub-frames duration (duty cycle), we propose a proportional power boosting for $\pi/2$-BPSK as follows.

$$P = \min\{P_{\max}, 10\log_{10} N_{\mathrm{RB}} + P_0 + \alpha \mathrm{PL}\} + \delta_{\mathrm{boost}}$$

- For a 50% duty-cycle scenario, i.e., when there are 50% of uplink sub-frames in a radio frame, $\delta_{boost} = 3$ dB.
- For a 25% duty-cycle scenario, $\delta_{\mathrm{boost}} = 6$ dB.
- For a 25–50% duty-cycle scenario, $\delta_{\mathrm{boost}} = 3$–6 dB.

Note that in all the above proposed power boosting scenarios, the average user transmit power over time does not exceed the existing $P_{\max}$ (= 23 dBm) power-limit.

1 ***Remark***

Since the large-cell scenario is noise limited, the increased transmit power with proposed power boosting directly translates to an improvement in the SNR of the link. Thus, the proposed power boosting improves coverage for the cell-edge users.

4.2.3 Resource allocation

Typically, a scheduler allocates the resources based on the weightage/reward assigned to a particular user. In real life, this weightage can be defined to ensure proportional fairness among the users, equal allocation to all users, biased allocation to priority users, or maximum throughput achieving allocation, etc. For example, let a vector W be of size $1 \times U$, where each element $W(i)$ represents reward of the ith user, U represents the number of users attached to the sector, and Γ_{RBs} is the total number of available resource blocks. A heuristic way of allocating resources to the users can be defined as follows.

- Equal resource allocation:

$$W(i) = \frac{1}{U}$$

  The scheduler allocates $W(i) \times \Gamma_{\text{RBs}}$ to each attached user.
- Proportional Fair:

$$W(i) = \frac{R^i(t)}{R^i_{\text{avg}}(t)},$$
$$R^i_{\text{avg}}(t) = \left(\frac{F-1}{F}\right) R^i_{\text{avg}}(t-1) + \frac{1}{F} R^i(t)$$

where F is the averaging window length and R^i *and* R^i_{avg} are the instantaneous and average rates of ith user. The scheduler allocates $W(i) \times \Gamma_{\text{RBs}}$ to each attached user.

Note that when the user transmits at the maximum power on one resource block, the user still observes SNRs as low as -15 dB in a large-cell scenario (shown in Sect. 3.2). Hence, most of the time, users are capable of transmitting on less number of resource blocks in a large-cell site. The scheduling algorithm should consider this limitation while allocating the resources to a user. Otherwise, the user will transmit at maximum power and still finds the transmission unsuccessful most of the time. Thus, we define the maximum resource blocks that can be allocated to a user ($N^{\max}_{\text{RB}}$) based on the power control in (4) as follows.

$$N^{\max}_{\text{RB}} = 10^{\frac{P_{\max} - P_0 - \alpha \text{PL}}{10}} \tag{5}$$

We propose to allocate resources to the users in two steps. In the first step, each user is assigned with $\left\lfloor \min(W(i) \times \Gamma_{\text{RBs}}, N^{\max}_{\text{RB}}(i)) \right\rfloor$ resource blocks. In the next step, we allocate the left-over bandwidth to the other users that are capable of transmitting in more number of resource blocks.

1 ***Remark***

This way, the proposed allocation ensures that the whole bandwidth is filled, while each user is allocated with resource blocks based on their transmitting capability.

Algorithm 1: Proposed power-scaling and resource allocation

Input : W, Γ_{RBs}, PL, P0, α, δ_{boost}
Output: Resource allocation and power-setting: $\mathrm{N_{RB}}$, P

A. Restricting the allocation to maximum possible resource blocks for each user

i = 1; /* i represents the user index */
for i = 1, . . . , U **do**
  $\mathrm{N_{RB}^{max}(i)} = 10^{\frac{\mathrm{P_{max}} - \mathrm{P_0} - \alpha \mathrm{PL(i)}}{10}}$
  $\mathrm{N_{RB}(i)} = \lfloor \min(\mathrm{W(i)} \times \Gamma_{\mathrm{RBs}}, \mathrm{N_{RB}^{max}(i)}) \rfloor$
end

B. Allocating left-over resource blocks to the other users

while $\sum_{\mathrm{i=1}}^{\mathrm{U}} \mathrm{N_{RB}(i)} < \Gamma_{\mathrm{RBs}}$ **do**
  for i = 1, . . . , U **do**
    if $\mathrm{N_{RB}(i)} + 1 \leq \mathrm{N_{RB}^{max}(i)}$ and $\left(\sum_{\mathrm{i=1}}^{\mathrm{U}} \mathrm{N_{RB}(i)}\right) + 1 \leq \Gamma_{\mathrm{RBs}}$ **then**
      $\mathrm{N_{RB}(i)} = \mathrm{N_{RB}(i)} + 1$
    end
  end
end

C. Power-scaling appropriately for each user

for i = 1, . . . , U **do**
  $\mathrm{P(i)} = \min\{\mathrm{P_{max}}, 10\log_{10}\mathrm{N_{RB}(i)} + \mathrm{P_0} + \alpha \mathrm{PL}\}$
  if $\mathrm{P(i)} = \mathrm{P_{max}}$ and modulation is $\pi/2 - \mathrm{BPSK}$ **then**
    $\mathrm{P(i)} = \mathrm{P(i)} + \delta_{\mathrm{boost}}(\mathrm{i})$
  end
end

In Algo. 1, we present the implementation of the power boosting and resource allocation procedures in detail.

4.3 Proposed code rates

In 4G-LTE/5G-NR, the channel quality index (CQI) is a metric reported by user about the SNRs observed in the downlink. Based on this CQI report, the BS assigns the modulation and coding scheme (MCS) and allocates resource blocks to the user. The user reports CQI as a four-bit value, and thus, it can convey the channel quality in 16 levels/steps. For this reason, the possible SNR values are grouped into 16 entries, and a one-to-one mapping is performed with these 16 CQI levels or code rates. Similarly, the MCS is conveyed as a five-bit value to the user, and thus, the MCS table has 32 entries. In Table 3, we have presented the CQI table used in the current 4G-LTE/5G-NR systems. As shown in Table 3, the minimum SNR for the least possible CQI is −6.9 dB. In a large-cell scenario, the operating SNRs are much lower, and hence, we need new CQI entries. Similar to the new CQI entries at lower SNRs, we need new MCS entries for the lower SNRs appropriately. Motivated by this, in this section, we present a procedure for extension of CQI and MCS tables to support lower SNRs.

4.3.1 CQI tables

The current 5G-NR CQI table is presented in Table 3. The CQI entries are defined with equal spacing considering an SNR range of −6.9 to 20 dB. Each CQI entry is separated by

Table 3 CQI table from the existing LTE/NR specifications

CQI	Modulation	Code rate × 1024	Efficiency	SNR in dB [BLER = 0.1]
0	Out of range			
1	QPSK	78	0.1523	−6.9
2	QPSK	120	0.2344	−5.10
3	QPSK	193	0.3770	−3.15
4	QPSK	308	0.6016	−1.25
5	QPSK	449	0.8770	−0.8
6	QPSK	602	1.1758	2.7
7	16QAM	378	1.4766	4.7
8	16QAM	490	1.9141	6.55
9	16QAM	616	2.4063	8.6
10	64QAM	466	2.7305	10.4
11	64QAM	567	3.3223	12.3
12	64QAM	666	3.9023	14.2
13	64QAM	772	4.5234	15.9
14	64QAM	873	5.1152	17.85
15	64QAM	948	5.5547	19.85

1.892 dB from one another [24]. The CQI table considers QPSK, 16 QAM, and 64 QAM modulation schemes. Based on the link-level simulations, the block error rates (BLER) are calculated for each modulation scheme and varying code rates. At each SNR entry in the CQI table, the code rate is chosen such that the BLER at that code rate is 10%. While adding new entries into the table for large-cell sites, we have also adopted a similar procedure. Since the users in large-cell sites observe poor SNRs, we removed the higher modulation scheme (64 QAM) and introduced entries with $\pi/2$-BPSK modulation. Further, instead of relying on the link-level simulations for BLER, we have used the BLER approximation formulated in [25]. In [25], the authors have performed link-level simulations and have formulated the approximation equation for mapping the spectral efficiencies and SNRs. We have used this equation to decide the code rates for the new CQI entries, and the same is presented in (6).

$$\begin{aligned} \mathrm{SE} = {} & 9.6 \times 10^{-5} \times \mathrm{SNR}^3 + 0.00533232 \times \mathrm{SNR}^2 \\ & + 9.89 \times 10^{-2} \times \mathrm{SNR} + 0.629993 \end{aligned} \tag{6}$$

The approximation in (6) maps the SNR to a spectral efficiency such that the desired BLER is 10%. Thus, using (6), we calculate the code rates and the spectral efficiencies at every 1.892 dB interval and formulate Table 4. Since the CQI has to be conveyed through 4 bits, we introduce six new CQI entries for the lower SNRs by removing the CQI entries with 64 QAM. Note that the CQI entries from 1 to 12 in Table 4 are allowed to be either QPSK/BPSK, $q = 1$ for $\pi/2$-BPSK, and $q = 2$ for QPSK. For a given number of resource block allocation, the QPSK is allowed to have half the code rate of the BPSK, and thus, both the entries will have the same spectral efficiencies. However, when $\pi/2$-BPSK is activated, as mentioned earlier, the user can transmit with more power. A similar extension has to be carried out for including the MCS entries for low SINRs as well. Next, we present the MCS tables for the large-cell sites.

4.3.2 MCS tables

The MCS table for uplink, as per current NR specifications [26], is presented in Table 5. The entries in Table 5 are carried out as follows. Initially, all the CQI entries (modulation choices and their respective code rates) in Table 3 are included in Table 5 as well. The relation between code rate (or spectral efficiency) of CQI entries in Table 3 and MCS entries in Table 5 can be formulated as follows.

$$\mathrm{MCS}(2 \times i + 2) = \mathrm{CQI}(i), \quad \forall\, i = 1, \ldots, 12$$

The other entries in Table 5 are obtained by interpolating the adjacent code rates as follows.

$$\mathrm{MCS}(2 \times \mathrm{i} + 3) = \frac{\mathrm{MCS}(2 \times i + 2) + \mathrm{MCS}(2 \times i + 4)}{2}, \quad \forall\, i = 1, \ldots, 12$$

For example, the spectral efficiencies of CQI 1 and 2 in Table 3 are 0.1523 and 0.2344, respectively. They are included as MCS 4 and 6 in Table 5 with same spectral efficiencies, respectively. Then, the MCS 5 is included in Table 5 such that it has spectral efficiency equal to average of the spectral efficiencies of MCS 4 and 6, i.e., $((0.1523 + 0.2344)/2 = 0.1934)$. The same holds for all the other MCS entries as well.

We follow a similar procedure for the new MCS entries to accommodate lower code rates in a large-cell scenario. We remove the higher modulation entries and include all the code rates from the proposed CQI in Table 4. We then interpolate the other entries, as mentioned earlier. The newly formed MCS table is presented in Table 6.

1 ***Remark***

Thus, the proposed CQI and MCS tables with lower code rates can ensure communication to users with SNRs as low as −17.7 dB with 10% BLER.

Next, we propose a novel scaling of transport blocks to improve the user throughputs.

4.4 Proposed transport-block scaling

The transport block is the actual data-carrying payload transmitted by the user in the uplink. The user attaches a cyclic-redundancy check (CRC)-based parity bits to the payload before channel encoding and transmitting. This helps the receiver perform a CRC check after decoding the payload and ensure all the decoded bits are error-free. However, in a large-cell scenario, the users are limited by transmit power and hence are capable of transmitting on fewer resource blocks most of the time. In such scenarios, the transport block will be of smaller size, and adding CRC parity bits in every slot will be additional overhead. To address this issue, we propose a transport-block scaling procedure as follows.

In case of eMBB transmissions, we calculate a transport block for multiple slots and attach the CRC parity bits once per this transport block transmitted over multiple slots. In case of voice-over-IP (VoIP) transmissions, typically, the transport block is of size 320 bits. In each slot of VoIP transmissions, the CRC parity bits are attached to

Table 4 Proposed CQI table for coverage enhancements

CQI	Modulation	Code rate × 1024	Efficiency	SNR in dB [BLER = 0.1]
0	Out of range			
1	QPSK/BPSK	11/q	0.0107	−17.7
2	QPSK/BPSK	14/q	0.0136	−15.9
3	QPSK/BPSK	21/q	0.0205	−14.1
4	QPSK/BPSK	36/q	0.0351	−12.3
5	QPSK/BPSK	63/q	0.0615	−10.5
6	QPSK/BPSK	106/q	0.1036	−8.7
7	QPSK/BPSK	156/q	0.1523	−6.9
8	QPSK/BPSK	240/q	0.2344	−5.10
9	QPSK/BPSK	386/q	0.3770	−3.15
10	QPSK/BPSK	716/q	0.6016	−1.25
11	QPSK/BPSK	898/q	0.8770	−0.8
12	QPSK/BPSK	1204/q	1.1758	2.7
13	16QAM	378	1.4766	4.7
14	16QAM	490	1.9141	6.55
15	16QAM	616	2.4063	8.6

the payload. In such scenarios, instead of transmitting the payload with CRC in each slot, we propose to attach a single CRC to the payload and rate-match (or repeat) the data over multiple slots. A pictorial representation of the proposed procedure is presented in Fig. 7. Further, in both the above scenarios, in case of an unsuccessful transmission of a transport block, we allow the transmitter to perform regular hybrid-ARQ procedures on this multi-slot transport-block transmission. We explain the significance of the proposed algorithm with an example as follows.

Consider a user allocated with one physical resource block, where 2 and 12 OFDM symbols in the slot are allocated for reference signals and data transmissions, respectively. Thus, there are $12 \times 12 = 144$ resource elements available for the user's data transmission. In the case of QPSK modulation, 2 bits can be transmitted in each resource element, and hence, the user can transmit 288 bits in total. The least possible transport-block size as per the current 5G-NR specifications is 24 bits. The user appends 16 bits of CRC, and thus, the effective payload size is 40 bits before the channel encoding. When the user performs rate matching and fits the data into the available 144 resource elements, the effective code rate of the transmission is $40/288 = 0.139$. In the case of the proposed algorithm, we append CRC once per four slots, and thus, the transport block will be of size $24 \times 4 = 96$. Further, a total of $144 \times 4 = 576$ resource elements are available for the transmission. Thus, with the proposed scheme, the effective code rate for the transmission is $112/1152 = 0.097$. This decrement in the code rate with the proposed scheme significantly improves the user's link performance.

Further, by allocating fewer resource blocks to the user in each uplink sub-frame, the network operators can significantly increase the cellular coverage. In the uplink, the available transmit power is spread across the allocated resource blocks. Consider allocating fewer resource blocks to the cell-edge user at any time instant and

Table 5 Existing MCS table

MCS	Modulation	Code rate × 1024	Efficiency
0	q	60/q	0.0586
1	q	80/q	0.0781
2	q	100/q	0.0977
3	q	128/q	0.1250
4	q	156/q	0.1523
5	q	198/q	0.1934
6	2	120	0.2344
7	2	157	0.3066
8	2	193	0.3770
9	2	251	0.4902
10	2	308	0.6016
11	2	379	0.7402
12	2	449	0.8770
13	2	526	1.0273
14	2	602	1.1758
15	2	679	1.3262
16	4	378	1.4766
17	4	434	1.6953
18	4	490	1.9141
19	4	553	2.1602
20	4	616	2.4063
21	4	658	2.5703
22	4	699	2.7305
23	4	772	3.0156
24	6	567	3.3223
25	6	616	3.6094
26	6	666	3.9023
27	6	772	4.5234
28	q	Reserved	
29	2	Reserved	
30	4	Reserved	
31	6	Reserved	

implementing the proposed algorithm of transmitting the transport block across multiple slots. In such a scenario, the cell-edge user can comparatively transmit more power on each allocated resource block and reduce the error rate of data transmissions. Additionally, there is also CRC overhead reduction which further improves the cellular coverage. This gain in the transmit power can be explained as follows. Let the number of resource blocks allocated and the repetitions assigned for the data transmission in the uplink be N_{RB} and N_{rep}, respectively. Then, the transmit power on each resource block is formulated as

$$P_{\mathrm{RB}} = P_{\mathrm{tx}} - 10\log(N_{\mathrm{RB}}) \tag{7}$$

In the proposed algorithm, we avoid the repetitions and assign resource blocks as follows

Table 6 Proposed MCS table

MCS	Modulation	Code rate × 1024	Efficiency
0	q	11/q	0.0107
1	q	12/q	0.0117
2	q	14/q	0.0136
3	q	17/q	0.0166
4	q	21/q	0.0205
5	q	28/q	0.0273
6	q	36/q	0.0351
7	q	49/q	0.0478
8	q	63/q	0.0615
9	q	84/q	0.0820
10	q	106/q	0.1036
11	q	131/q	0.1279
12	q	156/q	0.1523
13	q	198/q	0.1934
14	2	120	0.2344
15	2	157	0.3066
16	2	193	0.3770
17	2	251	0.4902
18	2	308	0.6016
19	2	379	0.7402
20	2	449	0.8770
21	2	526	1.0273
22	2	602	1.1758
23	2	679	1.3262
24	4	378	1.4766
25	4	434	1.6953
26	4	490	1.9141
27	4	553	2.1602
28	4	616	2.4063
29	q	Reserved	
30	2	Reserved	
31	4	Reserved	

$$N_{\mathrm{RB}}^{'} = \begin{cases} \lfloor N_{\mathrm{RB}}/N_{\mathrm{rep}} \rfloor, & \text{if } N_{\mathrm{RB}} \geq N_{\mathrm{rep}}, \\ \lceil N_{\mathrm{RB}}/N_{\mathrm{rep}} \rceil, & \text{if } N_{\mathrm{RB}} < N_{\mathrm{rep}}. \end{cases} \tag{8}$$

Thus, the gain in the transmit power with the proposed algorithms is proportional to the number of repetitions.

1 *Remark*

The proposed algorithm reduces the overhead because of the parity bits, improves the cellular coverage by allowing more transmit power on each resource block, and, thus, significantly improves the user throughput.

Next, we present the simulation set up and explain the results in detail.

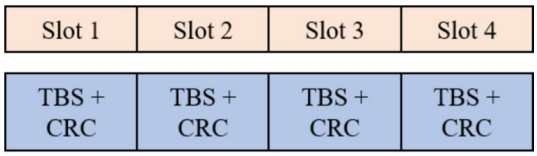

(a) Transport block allocation with the existing 3GPP scheme

(b) Transport block allocation with the proposed 2 slot aggregation

Fig. 7 Comparison of the proposed transport-block scaling with the existing 3GPP scheme

5 Simulation results and discussion

In this section, we initially present the calibration of the system-level simulator used for the evaluation. Then, we explain the system-level and link-level simulation procedures for evaluating all the proposed enhancements and discuss the results in detail.

5.1 Calibration of system-level simulator

The simulation parameters considered for the calibration are shown in Table 7 [28]. We initially drop the users randomly in each sector following the user distribution presented in Table 7. We then generate the distant dependent path loss and shadow fading between each user and BS considering LMLC path loss model in [15]. For the fast-fading channel, we implement the rural macro (RMa) model as per 3GPP specifications [27]. We calculate the reference signal received power ($\mathrm{RSRP}_{b,u}$) for each user (u) from each BS (b) as follows [17].

$$\mathrm{RSRP}_{b,u} = P_{\mathrm{tx}}.\mathrm{PL}_{b,u}.\mathrm{SF}_{b,u}.\sum_{k} = 1_{\mathrm{sc}}^{N}(|H_{b,u,k}|^2) \tag{9}$$

where P_{tx} is the BS transmit power; $\mathrm{PL}_{b,u}$, $\mathrm{SF}_{b,u}$, and $H_{b,u,k}$ are path loss, shadow fading, and channel experienced by the user u from the BS b on sub-carrier k, respectively. We then attach every user to a BS from which it has maximum RSRP value. The remaining BSs are considered as interference for that user.

The wideband signal-to-interference-plus-noise power ratio (SINR) is defined as the ratio of the received signal power from the attached BS to the interference from the other BSs plus noise. Thus, we calculate ($\mathrm{SINR}_{b,u}$) for each user as follows.

$$\mathrm{SINR}_{b,u} = \frac{\mathrm{RSRP}_{b,u}}{\sum_{b' \neq b} \mathrm{RSRP}_{b',u} + (kT \times \mathrm{BW})} \tag{10}$$

where u is the user index, b is the attached BS, k is the Boltzmann constant, T is the temperature, and BW is the bandwidth.

The coupling loss of a user is defined as the power loss in the received signal, as compared to the transmitted signal. It includes path loss, shadow fading, antenna gains, and

average small-scale fading. We calculate the coupling loss ($CL_{b,u}$) of a user (u) from its attached BS (b) as follows.

$$CL_{b,u} = RSRP_{b,u} - Pt_{BS} \tag{11}$$

In Figs. 8 and 9, we present the CDF of wideband SINR and coupling loss generated with our simulator and compare them against other companies' curves that participated in the 3GPP calibration activity [28]. The curves generated with our simulator completely align with the reference curves for both SINR and coupling loss.

5.2 System-level evaluation of proposed enhancements

The simulation parameters assumed for the evaluation of the proposed enhancements are presented in Table 8. We assume an inter-site distance of 30 km and consider two scenarios to capture the 4G-LTE/5G-NR deployments. In Scenario 1, we consider an operating carrier frequency of fc = 700 MHz and antenna configuration of 16 elements to suit the 4G-LTE deployment [16, 18]. In Scenario 2, we consider fc = 4 GHz and a 64 element antenna configuration to suit 5G-NR deployment [16, 18]. We also consider TDD configurations with 40% and 20% duty cycle for the evaluation. We perform the simulation with the existing 3GPP procedures and compare the performance against the proposed enhancements. All the other general parameters like small-scale fading, large-scale fading, user attach procedures, etc., are similar to the procedures followed in the calibration.

In Fig. 10, we present a pictorial overview of the simulation procedure. We initially drop 10 users randomly in each sector and perform the user attach procedure. Then, we consider an equal allocation of available resources to the attached users while evaluating the

Table 7 Simulation parameters for the calibration

Parameter	Value
Antenna at BS	$M \times N \times P = 8 \times 4 \times 2$
Antenna at UE	$M \times N \times P = 1 \times 2 \times 2$
Path loss model	RMa-LMLC as per [15]
Fast-fading model	RMa as per 3GPP TR 38.901 [27]
Inter-site distance	6 km
System bandwidth	10 MHz
User density	10 per sector
User distribution	40% indoor 40% outdoor 20% outdoor in-car
Mechanical/electrical tilt	90° in GCS/92° in LCS
BS/UE height	35 m/1.5 m
BS/UE transmit power (P_{tx})	46 dBm/23 dBm
BS/UE antenna gain	8 dBi/0 dBi
BS/UE noise figure	5 dB/7 dB
Interference modeling	Explicit
Thermal noise	−174 dBm/Hz
Sector boresight	30/150/270 degrees
User attachment	Based on RSRP
General parameters	Parameters not mentioned explicitly are as per [28]

existing 3GPP scheme. For the proposed enhancements case, we consider maximum transmit power based allocation presented in Sect. 4.2. We consider Tables 5 and 6 to assign MCS to the users while evaluating 3GPP scheme and proposed enhancements, respectively. We then set the transmit power to each user based on the power control mentioned in (4). In the proposed enhancements, we consider an additional power boosting based on the configured duty cycle for $\pi/2$-BPSK transmissions (discussed in Sect. 4.2). We then explicitly capture the interference from the users in other sectors and calculate the SINR at the receiver assuming a minimum mean-squared error (MMSE) equalization for both the scenarios. We also account for the channel estimation errors while calculating the SINR for each user. Based on this SINR, we decide ack/nack for the transmission. We continue this procedure until we reach the required simulation time and then generate the desired performance metrics.

Further, in real life, the channel estimation errors have a significant impact on the SINRs of users. Hence, while evaluating the SINR, the channel estimation errors have to be abstracted in the system-level simulations. Based on the approach mentioned in [29], we define the abstraction as follows.

$$\begin{aligned} y &= hx + n \\ \hat{h} &= yx^* \\ &= h + \hat{n} \\ E(\hat{h} - h) &= |E(x^* n)| \\ &= |x|^2 \sigma^2 = \frac{1}{\text{SNR}} \ (\because x \text{ is unit-modulus}) \\ \hat{h} &= h + \varepsilon, \varepsilon \sim \mathcal{N}\left(0, \frac{1}{\text{SNR}}\right) \end{aligned} \tag{12}$$

Thus, we consider an additional noise because of channel estimation error (ε), while calculating the interference for each user.

We then calculate the user throughput and cell throughput as follows.

$$\text{User Throughput} = \frac{\text{Bits delivered by the user}}{\text{Simulation time}} \tag{13}$$

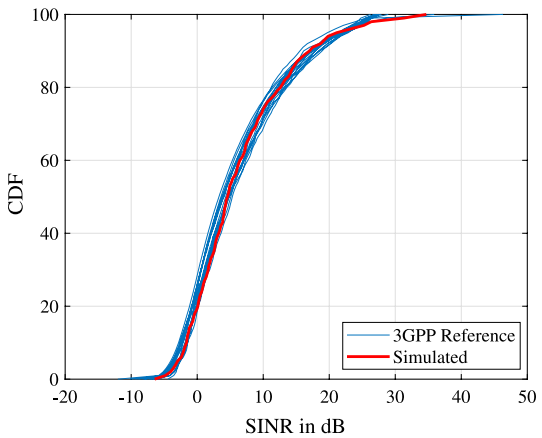

Fig. 8 Calibration of SINR with LMLC

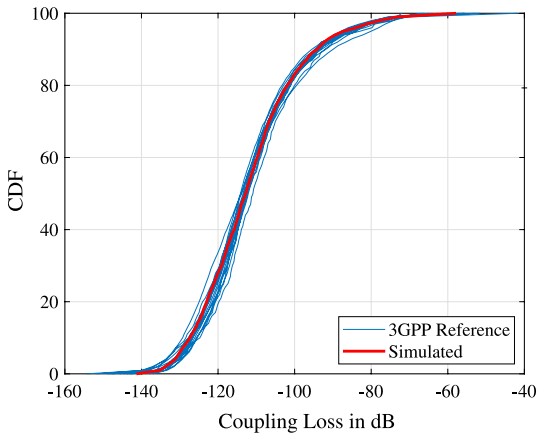

Fig. 9 Calibration of coupling loss with LMLC

Table 8 Simulation parameters for system-level evaluation

Parameter	Scenario 1	Scenario 2
Carrier frequency (fc)	700 MHz	4 GHz
Antenna at BS [$M \times N \times P$]	$4 \times 2 \times 2$	$8 \times 4 \times 2$
# TxRUs per sector	4	8
Antenna at UE	1	
Inter-site distance	30 km	
Receiver type	MMSE	
Resource allocation	Equal allocation to attached users	
Duty cycle	Configuration 1: 40% UL	
	Configuration 2: 20% UL	
Other parameters	Parameters not explicitly	
	Mentioned here are as per Table 7	

$$\text{Cell Throughput} = \frac{\text{Bits delivered by all the users in a sector}}{\text{Simulation time}} \tag{14}$$

In Figs. 11 and 12, the CDF of SINR is presented for the configurations of 40% and 20% duty cycle, respectively. In both the figures, fc = 700 MHz represents a 4G-LTE scenario, and fc = 4 GHz represents a 5G-NR scenario. With an increase in the carrier frequency, the user observes comparatively more path loss. However, with higher frequency, the BS can accommodate more antenna elements and compensate for this path loss. Thus, despite more path loss, the SINR values are better for the fc = 4 GHz scenario because of the 64 antenna elements at the BS. Further, when compared to the 3GPP scheme, with the proposed enhancements, the user can transmit with an additional $\delta_{\text{boost}} = 3$ dB for 40% duty-cycle and $\delta_{\text{boost}} = 6$ dB for 20% duty-cycle configurations, respectively. Since large-cell sites are noise limited, this additional transmission power directly improves the SINR values, as shown in Figs. 11 and 12.

In Figs. 13 and 14, the CDF of user throughput is presented for 40% duty-cycle and 20% duty-cycle configurations, respectively. The throughput values observed by the

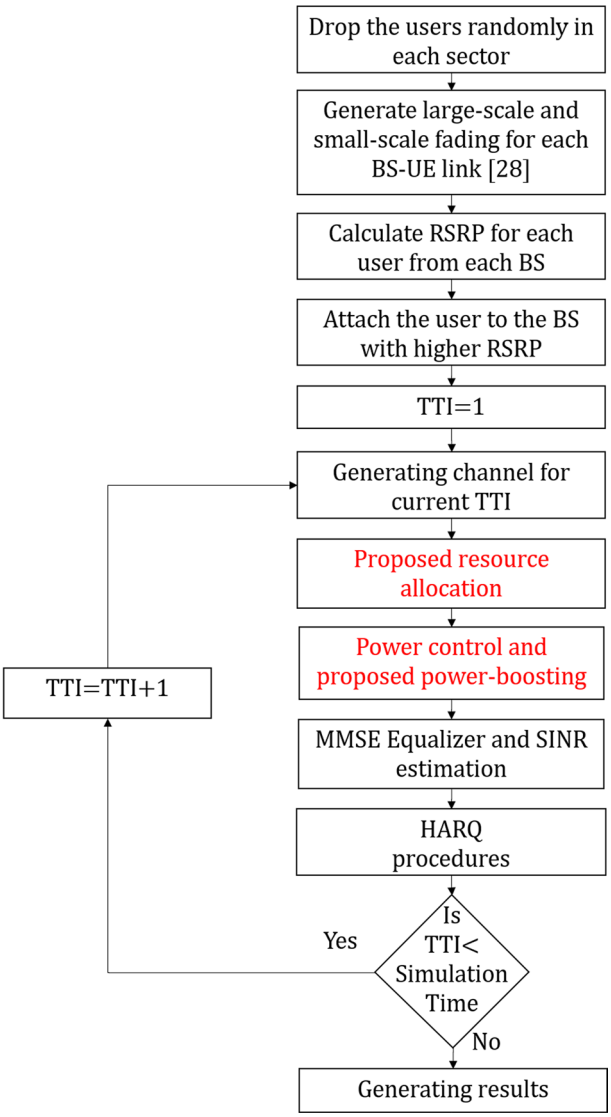

Fig. 10 Overview of the simulation procedure

users have a similar trend as that of the SINR values. Thus, the proposed enhancements significantly improve user throughput. Note that compared to 40% duty-cycle configuration, the throughput values are low in the 20% duty cycle because of the fewer active uplink sub-frames.

We have summarized the cell-edge, mean, and median throughput values for all the scenarios in Table 9. In Configurations 1 and 2, the proposed enhancements achieve a close to 2 times and 4 times improvement in network capacity, respectively. For the VoIP transmissions, a target throughput of 16 Kbps is required for the cell edge [18]. Our proposed enhancements achieve the target cell-edge throughput for both the 40% and 20% duty-cycle scenarios. Thus, the proposed enhancements can significantly improve cell-edge coverage and achieve target data rates in extremely large-cell sites.

5.3 Link-level evaluation of proposed enhancements

The simulation parameters assumed for the link-level evaluation are presented in Table 10. The evaluation is carried out as follows. In the case of the existing 3GPP scheme, we assume one resource block allocation, calculate the transport-block size for MCS = 0, attach a CRC to the transport block in each slot, and perform the link-level evaluation. In the case of the proposed enhancements, we calculate the transport-block size to fit in 2 slots and 4 slots. We then attach a CRC to the transport block once for the payload transmitted in the 2 slots and 4 slots, respectively, and perform the link-level evaluation. In the proposed enhancements scenario, reduced CRC overhead improves the code rate for the user, and thus, achieves better performance. In Fig. 15, we compare the BLER performance of the proposed enhancements against the 3GPP scheme. With a slot aggregation of 4, the reduced CRC overhead results in close to 3 dB improvement. This 3 dB gain results in a coverage improvement similar to the 3 dB power boosting with the $\pi/2$-BPSK presented in Sect. 5.2. Further, note that the improved performance with the transport-block scaling is significant at the lower code rates and smaller transport-block sizes. This is the scenario in case of the large-cell sites, as the cell-edge users typically transmit at fewer resource blocks and operate at lower code rates. Thus, our proposed enhancements can significantly improve the coverage when compared to the existing 3GPP schemes.

Further, we have evaluated the proposed enhancements for both VoIP and eMBB scenarios. In Fig. 16, we have presented the comparison of BLER with the 3GPP scheme and the proposed enhancements for the VoIP scenario. We have considered the "DDDSU" format, a code rate of 0.1533, and the transport-block size of 352 bits for the transmissions. For evaluating the 3GPP scheme, we consider eight resource blocks for the user. We then repeat the transport block eight times over time since we have eight uplink slots in a 20 ms duration. While implementing the proposed enhancements, we assign only one resource block and consider the resources available in all the eight uplink slots to obtain one transport-block size. We then append one CRC and transmit it over eight uplink slots. As shown in Fig. 16, with the proposed enhancements, there is a decrease in the number of repetitions by a factor of eight, and hence, there will be a degradation of 7 dB in the performance at the 2% BLER. However, note that we are transmitting on the

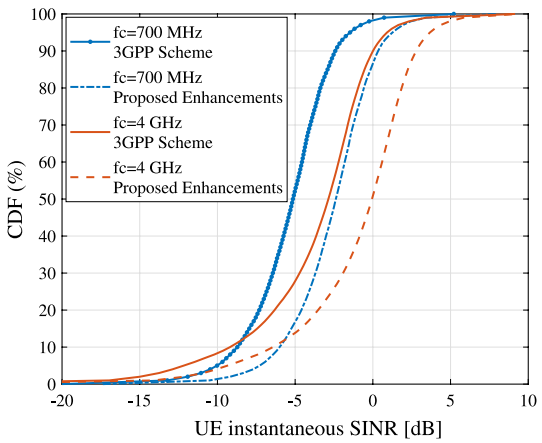

Fig. 11 Uplink SINR CDF with 40% duty cycle

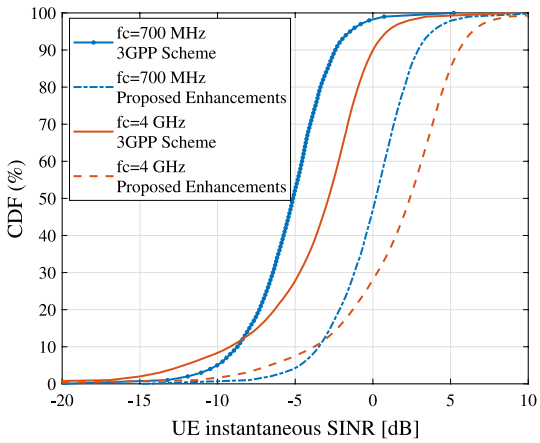

Fig. 12 Uplink SINR CDF with 20% duty cycle

Table 9 Summary of throughput results

		Configuration 1 40% duty cycle		Configuration 2 20% duty cycle	
		3GPP scheme	**Proposed enhancements**	**3GPP scheme**	**Proposed enhancements**
Scenario 1 fc = 700 MHz	5% user throughput	20.50 Kbps	39.26 Kbps	10.25 Kbps	35.42 Kbps
	50% user throughput	45.71 Kbps	94.86 Kbps	22.85 Kbps	79.56 Kbps
	Mean user throughput	53.64 Kbps	103.8 Kbps	26.82 Kbps	84.61 Kbps
	Mean cell throughput	536.4 Kbps	1.038 Mbps	268.2 Kbps	846.1 Kbps
Scenario 2 fc = 4 GHz	5% user throughput	12.26 Kbps	21.00 Kbps	6.130 Kbps	21.79 Kbps
	50% user throughput	74.47 Kbps	142.2 Kbps	37.23 Kbps	100.4 Kbps
	Mean user throughput	83.75 Kbps	149.2 Kbps	41.87 Kbps	104.9 Kbps
	Mean cell throughput	837.5 Kbps	1.492 Mbps	418.7 Kbps	1.049 Mbps

lesser number of resource blocks in the proposed scheme. This helps the user increase the transmit power by 9 dB, thus improving the cell coverage. We have used this link-level evaluation of VoIP and have carried out the link budget evaluation to quantify the improvement in the cell coverage. As shown in Table 11, the proposed enhancements achieve an improvement of 452 m in the cell radius. Further, note that with the proposed scheme, we are using 12.5% (or one-eighth) of the resources as compared to the current 3GPP scheme. We have carried out a similar evaluation for the eMBB scenario considering the desired data rates as 100 Kbps. Similar to the VoIP scenario, we observe degradation in the link-level performance as shown in Fig. 17. However, with the increased transmit power available at the user, considering this link-level evaluation, in Table 11, we show an improvement of 158 m in the cell radius for the eMBB scenario. Thus, the proposed enhancements help in achieving significant improvement in the network performance and cell coverage.

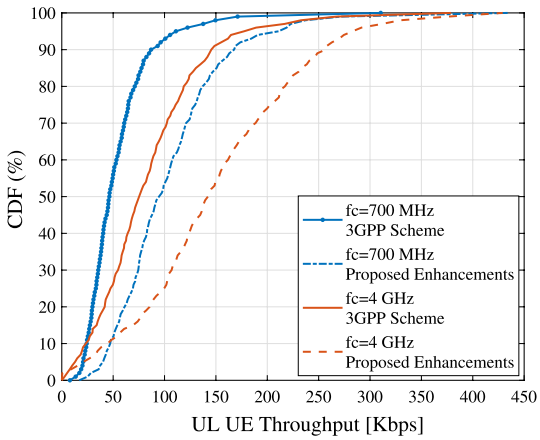

Fig. 13 User throughput CDF with 40% duty cycle

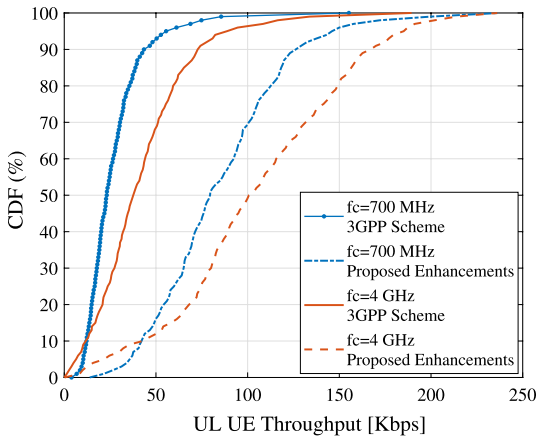

Fig. 14 User throughput CDF with 20% duty cycle

6 Conclusion and future work

In this paper, we have initially discussed various reasons why the latest cellular technologies could not improve rural connectivity in developing countries like India. We have shown that large-cell sites are a practically feasible solution to significantly enhance rural connectivity. We have performed a link budget evaluation of large-cell sites in a rural scenario and have shown that it is infeasible to achieve cellular coverage with the current LTE/NR specifications. To address this issue, we have proposed various enhancements related to waveform, code rates, resource allocation, and power control mechanisms. We have then evaluated the proposed algorithms through link and system-level simulations considering various configurations that are close to real-life deployment. Our proposed enhancements significantly improve the signal-to-noise power ratios and user throughputs compared to the existing 3GPP specifications. We have shown that our proposed solutions achieve minimum data-rate requirements specified by 3GPP in a large-cell scenario and have shown 2–4 times improvement in the cell-edge coverage. In the future, we plan to implement and validate the proposed enhancements on hardware test beds.

Table 10 Simulation parameters for link-level evaluation

Parameter	Value
System bandwidth	100 MHz
Sub-carrier spacing	30 KHz
Channel model	Rural, TDL-D, 30 ns
Waveform	DFT-s-OFDM
Modulation	QPSK
Coding rate	VoIP: 0.1533 eMBB:0.3008
Data rates	VoIP: 320 bits in 20 ms eMBB: 100 Kbps
Resource blocks	1
Repetitions	VoIP: 8 eMBB:4
Number of tx chains	1
Number of rx chains	4
Number of reference symbols in a slot	3
Number of data symbols in a slot	9
Frame structure	DDDSU

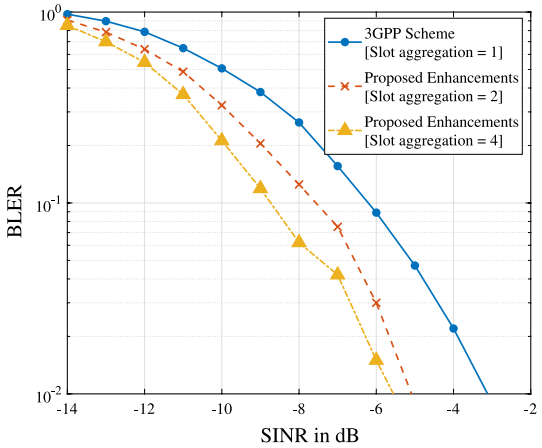

Fig. 15 Link-level evaluation of proposed transport-block scaling scheme

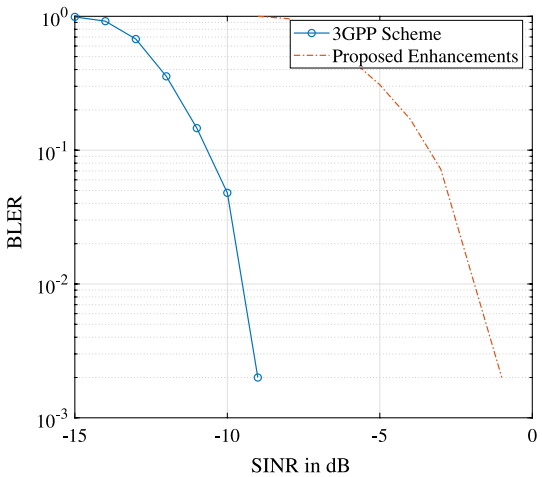

Fig. 16 VoIP evaluations used for calculating cell radius in Table 11

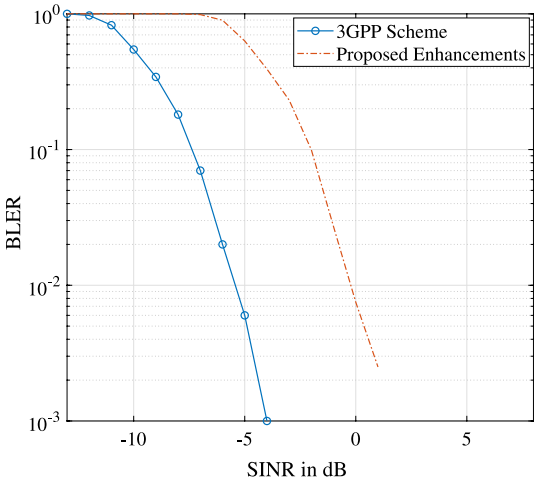

Fig. 17 eMBB evaluations used for calculating cell radius in Table 11

Table 11 Comparison of achievable cell coverage with the 3GPP scheme and proposed enhancements

Scenario	VoIP (m)	eMBB (m)
3GPP scheme	4240	4173
Proposed enhancements	4692	4331
Gain	452	158

Abbreviations

3GPP	3rd-generation partnership project
4G-LTE	4G-long-term evolution
5G-NR	5G-new radio
α	Fractional power control parameter
A_g	Antenna gain
BLER	Block error rate
BPSK	Binary phase shift keying
BS	Base station
CCDF	Complementary cumulative distribution function
CDF	Cumulative distribution function
CQI	Channel quality index
DFT-s-OFDM	Discrete Fourier transform spread orthogonal frequency division multiplexing
eMBB	Enhanced mobile broadband
GP	Gram-panchayat
IMT	International mobile telecommunications
ITU	International telecommunications union
LMLC	Low-mobility large cell
LoS	Line of sight
MCS	Modulation and coding scheme
MIMO	Multiple input multiple output
MMSE	Minimum mean squared error
mMTC	Massive machine-type communication
N_{BS}	Number of antennae at base station
N_{UE}	Number of antennae at user equipment
N_{RB}	Number of allocated resource blocks
NLoS	Non-line of sight
NF	Noise figure
OFDM	Orthogonal frequency division multiplexing
$P_{t_{BS}}$	Transmit power at base station
$P_{t_{UE}}$	Transmit power at user equipment
P_{max}	Maximum transmit power at user equipment
P_0	Power control parameter

PAPR	Peak-to-average power ratio
PL	Path loss
PRB	Physical resource block
QAM	Quadrature amplitude modulation
QPSK	Quadrature phase shift keying
RMa	Rural macro
SF	Shadow fading
SINR	Signal-to-interference-plus-noise power ratio
SNR	Signal-to-noise power ratio
TDD	Time division duplexing
UE	User equipment
URLLC	Ultra reliable low latency communication

Acknowledgements
Not applicable.

Author contributions
MPR and GKR have contributed equally to the current paper. All authors have extensively reviewed the proposed algorithms, simulated results, and structuring of the manuscript. All authors read and approved the final manuscript.

Funding
Not applicable.

Availability of data and materials
Not applicable.

Declarations

Competing interests
The authors declare that they have no competing interests.

Received: 12 September 2021 Accepted: 31 May 2022
Published online: 27 June 2022

References

1. Bharat Broadband Network Limited. http://www.bbnl.nic.in/. Last accessed 19 Oct 2020
2. ITU-R WP5D: IMT2020 developing countries discussion, TSDSI, Technical presentation. https://tsdsi.in/wp-content/uploads/2020/02/Presentation-to-Developing-Countries-Pamela-Kumar.pdf. Last accessed 19 Oct 2020
3. Nomor Research, Motivation paper and first results on Rel.17 Coverage Enhancements, 3rd Generation Partnership Project (3GPP), Technical document, RP-193080 (2020)
4. China Telecom, New SID on NR coverage enhancement, 3rd Generation Partnership Project (3GPP), Technical document, RP-193240 (2019)
5. 3GPP, User Equipment (UE) radio transmission and reception, 3rd Generation Partnership Project (3GPP), Technical specification, 38.101, v 16.3.0 (2020)
6. R. Ratasuk, et al., Coverage enhancement for M2M communications using LTE, in *Proceedings of International Conference on Telecommunications (ICT)* (2014), p. 482–486
7. S. Ravi, et al., Evaluation, modeling and optimization of coverage enhancement methods of NB-IoT, in *Proceedings of IEEE Annual International Symposium on Personal, Indoor and Mobile Radio Communications (PIMRC)* (2019), p. 1–7
8. G. Naddafzadeh-Shirazi et al., Coverage enhancement techniques for machine-to-machine communications over LTE. IEEE Commun. Mag. **53**(7), 192–200 (2015)
9. S. Xu, et al., Research on coverage enhancement of narrowband M2M communications based on unlicensed spectrum, in *Proceedings of IEEE 86th Vehicular Technology Conference (VTC-Fall)* (2017), p. 1–5
10. P. Annamalai et al., Constellation constraining-based coverage enhancement technique for MTC devices in LTE-A. IEEE Wirel. Commun. Lett. **5**(6), 596–599 (2016)
11. P. Annamalai et al., Coverage enhancement for MTC devices using reduced search Viterbi decoder across RATs. IEEE Commun. Lett. **20**(9), 1892–1895 (2016)
12. G. Liu et al., Coverage enhancement and fundamental performance of 5G: analysis and field trial. IEEE Commun. Mag. **57**(6), 126–131 (2019)
13. L. Cao, et al., VoLTE coverage improvement by HARQ and RLC segmentation when TTI bundling is ON, in *Proceedings of IEEE Information Technology, Networking, Electronic and Automation Control Conference* (2016), p. 371–375
14. Y. Song, et al., Adaptive digital beamforming for uplink coverage enhancement in 5G NR system, in *Proceedings of 27th Telecommunications Forum (TELFOR)* (2019), p. 1–4
15. ITU-R, Guidelines for evaluation of radio interface technologies for IMT-2020, International Telecommunications Union (ITU), Technical report, M.2412-0 (2017)
16. Nomor Research, Potential solutions on coverage enhancement for FR1, 3rd Generation Partnership Project (3GPP), Technical document, R1-2003938 (2020)
17. 3GPP, Study on 3D channel model for LTE, 3rd Generation Partnership Project (3GPP), Technical report, 36.873, v 12.7.0 (2017)

18. 3GPP, Study on NR coverage enhancements, 3rd Generation Partnership Project (3GPP), Technical document, R1-2005730 (2020)
19. Enhancing LTE cell-edge performance via PDCCH ICIC, Fujitsu, White paper. https://www.fujitsu.com/downloads/TEL/fnc/whitepapers/Enhancing-LTE-Cell-Edge.pdf. Last accessed 20 Oct 2020
20. 3GPP, NR; Physical channels and modulation, 3rd Generation Partnership Project (3GPP), Technical specification, 38.211, v 16.1.0 (2020)
21. M.S.A. Khan, et al., Low PAPR DMRS sequence design for 5G-NR Uplink, in *Proceedings of International Conference on Communication Systems Networks (COMSNETS)* (2020), p. 207–212
22. IITH, Comparison of pi/2 BPSK with and without frequency domain pulse shaping: results with PA model, 3rd Generation Partnership Project (3GPP), Technical document, R1-1701180 (2017)
23. 3GPP, NR; Physical layer procedures for control, 3rd Generation Partnership Project (3GPP), Technical specification, 38.213, v 16.1.0 (2020)
24. N. Li, et al., Extendable CQI table design for higher order modulation in LTE downlink transmission, in *Proceedings of IEEE/CIC International Conference on Communications in China (ICCC)* (2015), p. 1–5
25. B. Kim, Y. Yi, Method and device for feeding back channel state information in wireless access system supporting machine type communication, LG Electronics Inc, WIPO (PCT), WO2016175576A1 (2016)
26. 3GPP, NR; Physical layer procedures for data, 3rd Generation Partnership Project (3GPP), Technical specification, 38.214, v 16.1.0 (2020)
27. 3GPP, Study on channel model for frequencies from 0.5 to 100 GHz, 3rd Generation Partnership Project (3GPP), Technical report, 36.901, v 16.1.0 (2020)
28. 3GPP, [ITU-R AH 01] Calibration of self-evaluation, 3rd Generation Partnership Project (3GPP), Technical document, RP-180496 (2018)
29. 3GPP, WF on SRS estimation error modeling, 3rd Generation Partnership Project (3GPP), Technical document, R1-150867 (2015)

Publisher's Note